A semi-implicit, semi-Lagrangian, p-adaptive discontinuous Galerkin method for the rotating shallow water equations

Giovanni Tumolo[a], Luca Bonaventura[b], Marco Restelli[b]

[a] The Abdus-Salam International Center for Theoretical Physics, Trieste

[b] MOX – Modellistica e Calcolo Scientifico, Dip. Matematica, Politecnico di Milano

Presentation summary

- Motivation and overview.
- Shallow Water Equations
- Numerical formulation “ingredients” :
  - discontinuous Galerkin finite elements
  - semi-implicit time integration of stiff terms
  - semi-Lagrangian treatment of advective terms
  - p-adaptivity
- Numerical validation:
  - (rarefaction) Riemann problem
  - hydraulics benchmark
  - pure gravity wave propagation
  - geostrophic adjustment
  - Stommel test
- Conclusions and future plans

Motivation: new approaches to dynamical cores

- Long term goal: develop a new generation dynamical core for regional climate modelling (RegCM)

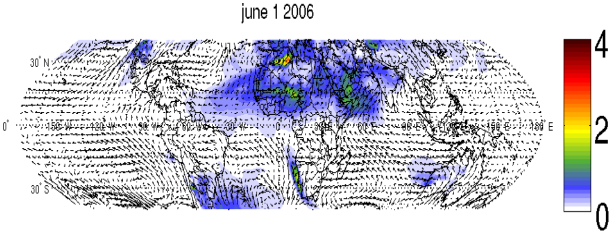

- Why do we need a new climate model dynamics ?
- Because, traditional models have serious limitations to satisfy all of the following properties:
  - Local and global conservation
  - High-order accuracy
  - High parallel efficiency
  - Resolution flexibility
  - monotonic (non-oscillatory) advection
- Discontinuous Galerkin (DG) based models have the potential to address all the above issues, but ...

Overview(I)

- ... when coupled to explicit time stepping, DG methods are affected by severe stability restrictions as polynomial order increases.
  Example: the RKDG (Cockburn-Shu, 1991) algorithm is stable provided the following condition holds:

  $$u\frac{\Delta t}{h} < \frac{1}{2k+1}$$

  where k is the polynomial degree; ($\Rightarrow$ for the linear case this implies a CFL limit $\frac{1}{3}$)
- ... moreover DG requires more degrees of freedom per element than Continuous Galerkin (CG) approach, thus more expensive.
- Short term goal: increase computational efficiency of DG by exploiting two techniques:
  - coupling to SI-SL techniques (no CFL conditions)
  - introduction of p-adaptivity (flexible degrees of freedom)

Overview(II): SI, SL and DG

Previously, the SI and SL techniques have been already coupled to DG, but only *separately*, up to now:

- SEMI-LAGRANGIAN time discretization of the advection equation $\Rightarrow$ SLDG
  (M. Restelli, L. Bonaventura, R. Sacco, J. Comput. Phys., 2006).
- SEMI-IMPLICIT time integration $\Rightarrow$ SIDG
  (M. Restelli, F. Giraldo, SIAM J. Sci. Comput. 2009).

The goal of this research is to combine *both* these techniques in order to write the first ever SISLDG scheme. In particular we want to:

- demonstrate feasibility of SISLDG approach in a simple modelling framework
- test the SISLDG algorithm on a series of idealised cases
- demonstrate the viability of p-adaptivity as an alternative/complement to mesh refinement(h-adaptivity)
- (in the future) apply this technology to a fully nonhydrostatic regional climate model (RegCM).

Shallow Water Equations (I): the testbed

- This equations set allows to highlight several important aspects of the complete multidimensional problem, indeed it contains all of the horizontal operators required in a complete atmospheric model

- it represents the standard first test of newly proposed schemes for atmospheric models.

Shallow Water Equations (II)

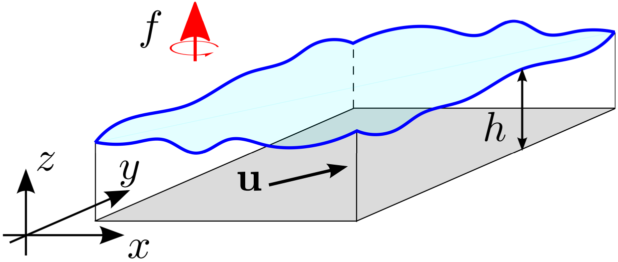

$h \ll L$

$h = \eta - b$

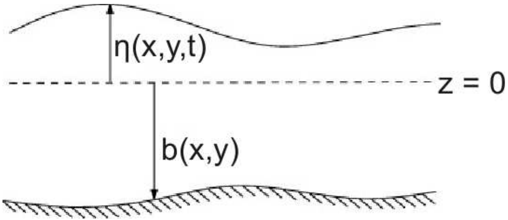

Shallow Water equations (III)

The Shallow Water Equations are:

$$\begin{aligned} \partial_t \eta &= -\nabla \cdot (h\mathbf{u}) \\ \partial_t \mathbf{u} + \mathbf{u} \cdot \nabla \mathbf{u} &= -g\nabla\eta + f\mathbf{k} \times \mathbf{u}. \end{aligned} \tag{1}$$

Problems in numerical solution of (1):

- mass conservation
- presence of gravity waves (*stiff* terms)
- constraint on the timestep size given by advection
- effects of Earth rotation
- possibile appearance of spurious modes for η and/or $\mathbf{u}$.

Numerical Formulation (I): DG

- DG methods are finite elements methods where a piecewise polynomial solution is sought that might be discontinuous in the passage from one element to the neighboring one:

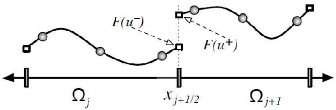

- Defined a (regular) tasselation $\mathcal{T}_h$ of domain Ω and chosen $\forall K \in \mathcal{T}_h$ two integers $p_K^\eta \geq 0$, $p_K^u \geq 0$, we are looking for approximate solution s.t.

$$
\begin{aligned}
\eta &\in H_h := \left\{ v \in L^2(\Omega) \,:\, v|_K \in \mathbb{Q}_{p_K^\eta}(K) \right\} \\
\mathbf{u} &\in U_h := \left\{ v \in L^2(\Omega) \,:\, v|_K \in \mathbb{Q}_{p_K^u}(K) \right\}^2 .
\end{aligned}
$$

- The choice of different polynomial orders for η and $\mathbf{u}$ is not necessary but $p^u = p^\eta + 1$ shows good stability properties for the Stokes problem.

Numerical formulation (II): SI

- For time discretization of stiff terms, associated with gravity wave propagation, a semi-implicit [1] method is used

$$
\begin{aligned}
\partial_t \eta &= -\theta \nabla \cdot \left(h^n \mathbf{u}^{n+1} \right) \\
&\quad -(1-\theta)\nabla \cdot (h^n \mathbf{u}^n) \\
\partial_t \mathbf{u} + \mathbf{u} \cdot \nabla \mathbf{u} &= -g\theta \nabla \eta^{n+1} + \theta f \mathbf{k} \times \mathbf{u}^{n+1} \\
&\quad -g(1-\theta)\nabla \eta^n + (1-\theta) f \mathbf{k} \times \mathbf{u}^n .
\end{aligned}
$$

- Notice that the implicit problem is linear.

[1] See e.g. [Casulli, 1990] and [Casulli, Cattani, 1994]

Numerical formulation (III): SL

For time discretization of advective terms the semi-Lagrangian method is used: for a generic scalar q we set

$$\partial_t q + \mathbf{u} \cdot \nabla q \approx \frac{1}{\Delta t} \left(q^{n+1} - q^{n,*} \right)$$

where $q^{n,*}(\mathbf{x}) = q^n(\mathbf{x}^*)$ and $\mathbf{x}^*$ is given by $\mathbf{X}(t^n)$, the solution backward in time of the trajectories problem

$$\frac{d\mathbf{X}}{dt} = \mathbf{u}(t, \mathbf{X})$$
$$\mathbf{X}(t^{n+1}) = \mathbf{x}$$

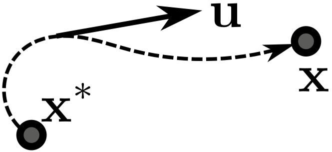

The stability of the semi-Lagrangian scheme is indipendent from the Courant number $C = |\mathbf{u}|\Delta t/\Delta x$.

Numerical formulation (IV): SISLDG

If the solution at time level t^n is known, the resulting discrete formulation is given by:
find $(\eta^{n+1}, \mathbf{u}^{n+1}) \in H_h \times U_h$ such that, $\forall K \in \mathcal{T}_h$, $\forall(\phi, \psi) \in H_h \times U_h$,

$$\begin{aligned}
\int_K \phi\, h^{n+1} &= \int_K \phi\, h^n + \theta\Delta t \left(\int_K \nabla\phi \cdot h^n \mathbf{u}^{n+1} - \int_{\partial K} \hat{h}^n \hat{\mathbf{u}}^{n+1} \cdot \mathbf{n}_{\partial K} \right) \\
&\quad + (1-\theta)\Delta t \left(\int_K \nabla\phi \cdot h^n \mathbf{u}^n - \int_{\partial K} \hat{h}^n \hat{\mathbf{u}}^n \cdot \mathbf{n}_{\partial K} \right) \\
\int_K \psi \cdot \mathbf{u}^{n+1} &= \int_K \psi \cdot \mathbf{u}^{n,*} + \theta\Delta t \int_K \psi \cdot \left(-g\nabla_h h^{n+1} + f\mathbf{k} \times \mathbf{u}^{n+1} \right) \\
&\quad + (1-\theta)\Delta t \int_K \psi \cdot \left(-g\nabla_h h^{n,*} + f\mathbf{k} \times \mathbf{u}^{n,*} \right)
\end{aligned}$$

where the numerical fluxes are given by [2]

$$\hat{h} = \frac{1}{2}\left(h^L + h^R\right), \qquad \hat{\mathbf{u}} = \frac{1}{2}\left(\mathbf{u}^L + \mathbf{u}^R\right).$$

[2] See e.g. Bassi, Rebay 1997

Numerical formulation (V): ∇_h

Notice that the discrete gradient operator

$$\nabla_h : H_h \mapsto H_h$$

is defined by exploiting numerical fluxes as

$$\int_K \phi \cdot \nabla_h h = -\int_K \nabla \cdot \phi \, h + \int_{\partial K} \phi \cdot \mathbf{n}_{\partial K} \, \hat{h}$$

for each $\phi \in H_h^2$ and each $K \in \mathcal{T}_h$.

Numerical formulation (VI): fully discrete problem

If $\boldsymbol{\eta}^{n+1}$, $\boldsymbol{u}^{n+1}$ and $\boldsymbol{v}^{n+1}$ contain the coefficients of the expansions of $h^{n+1}, u^{n+1}, v^{n+1}$ over the basis functions

- $\boldsymbol{u}^{n+1}$ and $\boldsymbol{v}^{n+1}$ are expressed in terms of $\boldsymbol{\eta}^{n+1}$ from momentum equation and resulting expressions substituted into the continuity equations, (Casulli, JCP, 1990),
- discrete (vector) Helmholtz equation in the $\boldsymbol{\eta}^{n+1}$ unknown only is obtained:

$$
\begin{array}{ccccc}
 & & K_I^{WW}\boldsymbol{\eta}_{I_{WW}}^{n+1} & + & \\
 & +K_I^{SW}\boldsymbol{\eta}_{I_{SW}}^{n+1} & +K_I^{W}\boldsymbol{\eta}_{I_{W}}^{n+1}+ & K_I^{NW}\boldsymbol{\eta}_{I_{NW}}^{n+1} + & \\
+K_I^{SS}\boldsymbol{\eta}_{I_{SS}}^{n+1} + & K_I^{S}\boldsymbol{\eta}_{I_{S}}^{n+1} & +K_I\boldsymbol{\eta}_{I}^{n+1}+ & K_I^{N}\boldsymbol{\eta}_{I_{N}}^{n+1} & +K^{NN}\boldsymbol{\eta}_{I_N N}^{n+1} + \\
 & +K_I^{SE}\boldsymbol{\eta}_{I_{SE}}^{n+1} & +K_I^{E}\boldsymbol{\eta}_{I_{E}}^{n+1}+ & K_I^{NE}\boldsymbol{\eta}_{I_{NE}}^{n+1} + & \\
 & + & K_I^{EE}\boldsymbol{\eta}_{I_{EE}}^{n+1} & = & \\
 & = & \mathcal{N}_I^n & , &
\end{array}
$$

Numerical formulation (VII): fully discrete problem

- where the computational stencil for the semi-implicit step and the names of the elements surrounding the element K_I are

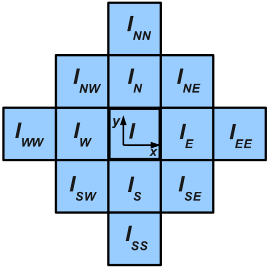

- sparse block structured non symmetric linear system solved by GMRES with diagonal preconditioning.

Numerical formulation (VII): p-adaptivity

- The use of discontinuous elements makes easy the introduction of adaptivity in space by locally varying the polynomial degree p_K.
- Since structured meshes of quadrilaterals are employed, tensor products of Legendre polynomials are a good choice as :
  - hierarchical : good for adaptive computation of the p_I;
  - orthogonal : fully diagonal mass matrix.
- Hence the representation for a model variable α becomes

$$\alpha(\boldsymbol{x})\big|_{K_I} = \sum_{k=1}^{p_I^\alpha+1} \sum_{l=1}^{p_I^\alpha+1} \alpha_{I,k,l}\psi_{I_x,k}(x)\psi_{I_y,l}(y).$$

with $I = (I_x, I_y)$ suitable multi-index.

- and the orthogonality of the basis implies:

$$\mathcal{E}^{tot} = \|P\alpha\|^2 = \sum_{k,l=1}^{p_I^\alpha+1} \alpha_{I,k,l}^2$$

where P is the L^2 projector onto the local polynomial subspace.

Orthogonality of the basis and p-adaptivity

- Then, for a given element $K_l \in \mathcal{T}_h$, the "*energy*" contained in the $r-$ th modal components of $\alpha\big|_{K_l}$ is given by:

$$\mathcal{E}^r := \sum_{max(k,l)=r} \alpha^2_{l,k,l}$$

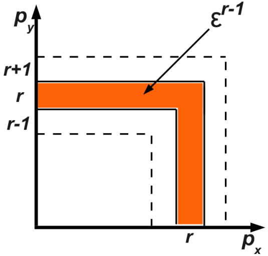

- while, for any integer $r = 1, \ldots, p_l^\alpha + 1$, the quantity

$$w_r = \sqrt{\frac{\mathcal{E}^r}{\mathcal{E}^{tot}}}$$

will measure the relative 'weight' of the $r-$th modal components of α with respect to the best approximation available for the L^2 norm of α.

p-adaptation algorithm

If α is a generic model variable, the following adaptation criterion is applied:

- Compute all model variables with p_{max} at initial time.
- *Given an error tolerance $\epsilon_l > 0$ for all $l = 1, \ldots, N$, at each time step repeat following steps:*

  1) *compute w_{p_i}*

  2.1) *if $w_{p_i} \geq \epsilon_i$, then*

    2.1.1) *set $p_i(\alpha) := p_i(\alpha) + 1$*

    2.1.2) *set $\alpha_{i,p_i} = 0$, exit the loop and go the next element*

  2.2) *if instead $w_{p_i} < \epsilon_i$, then*

    2.2.1) *compute $w_{p_i - 1}$*

    2.2.2) *if $w_{p_i - 1} \geq \epsilon_i$, exit the loop and go the next element*

    2.2.3) *else if $w_{p_i - 1} < \epsilon_i$, set $p_i(\alpha) := p_i(\alpha) - 1$ and go back to 2.2.1.*

p-adaptivity on the advective part: deformational flow

Smolarkiewicz advection test case:
Cone initial datum and advective velocity field defined by
$\psi(x,y) = 8 sin(4\pi x/L) cos(4\pi y/L)$

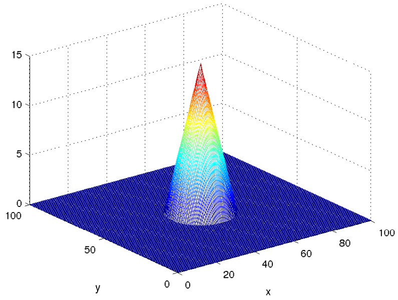

Figure: Initial datum for the Smolarkiewicz test.

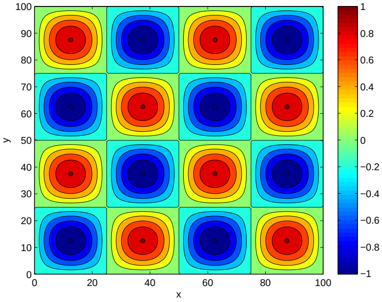

Figure: Advective velocity field for the Smolarkiewicz test.

p-adaptivity on the advective part: deformational flow

Smolarkiewicz advection test case:
effectiveness of $p-$adaptivity approach for complex pattern in 2D

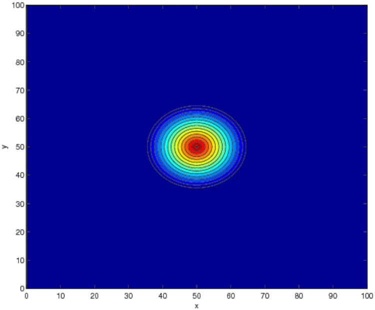

Figure: Solution contours evolution for $t \leq 300s$. $C_{vel} \approx 4$, $\epsilon = 10^{-2}$

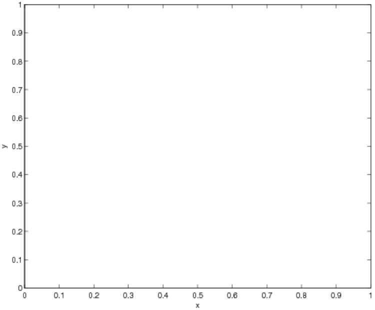

Figure: Local polynomial degrees evolution for $t \leq 300s$. $C_{vel} \approx 4$, $\epsilon = 10^{-2}$

Numerical Validation

Nonlinear unsteady test: rarefaction wave

Riemann problem for equations (1) with $f = 0$ and

$$h(x,0) = h_0,$$

$$u(x,0) = \begin{cases} u_l, & \text{if } x < 0 \\ u_l, & \text{if } x \geq 0 \end{cases}$$

where

$$h_0 = 2m, \quad u_r = -u_l = 0.5m/s$$

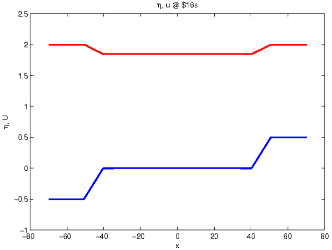

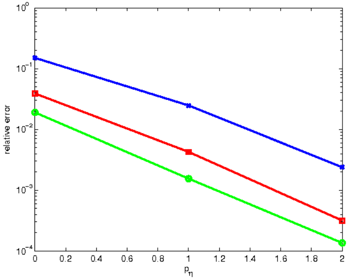

p_η	p_u	E_2^η	E_1^η	E_∞^η
0	1	3.89e-2	1.90e-2	1.50e-1
1	2	4.27e-3	1.55e-3	2.48e-2
2	3	3.18e-4	1.36e-4	2.39e-3

Non-constant bathymetry: subcritical steady channel flow over a parabolic bump

River hydraulics benchmark considered e.g. Rosatti et al., IJNMF, 2011, and Vazquez-Cendon, JCP 1998.

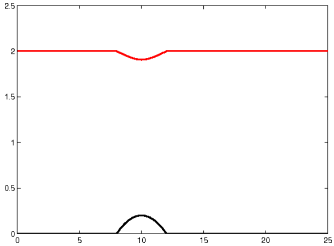

$$C_{vel} = \frac{u\Delta t}{\Delta x/p}$$

$$C_{cel} = \frac{|u+\sqrt{gh}|\Delta t}{\Delta x/p}$$

$$E_2^{std} = \frac{\left\|\eta^{n+1}-\eta^n\right\|_{L^2}}{\left\|\eta^{n+1}\right\|_{L^2}} \approx 10^{-14}$$

Δt	t step nb	C_{vel}	C_{cel}	E_∞^Q	E_2^Q
0.00625	48000	0.20	0.33	1.91e-5	1.33e-6
0.0125	24000	0.40	0.66	6.36e-4	3.85e-5
0.025	12000	0.80	1.32	1.23e-3	7.41e-5
0.05	6000	1.56	2.64	5.15e-3	3.75e-4
0.1	3000	3.10	5.31	7.46e-4	5.85e-5
0.2	1500	6.20	10.60	2.89e-3	2.18e-4

Gravity waves propagation

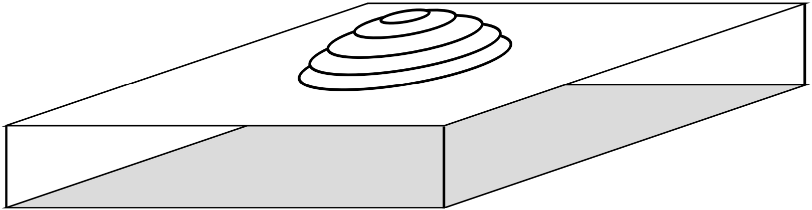

Initial datum: fluid at rest, free surface perturbation with circular symmetry (Gaussian bell); Square domain $(0\,km\,,10^4\,km)^2$, with free slip wall boundary conditions.

A regular mesh of 50×50 elements is employed.

Pure gravity wave (I): no rotation

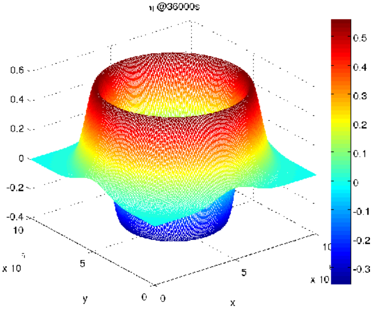

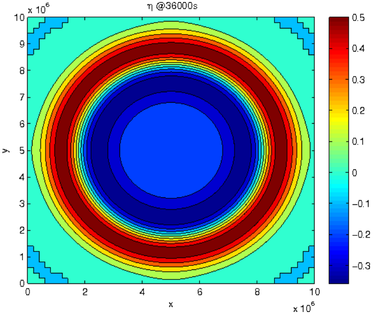

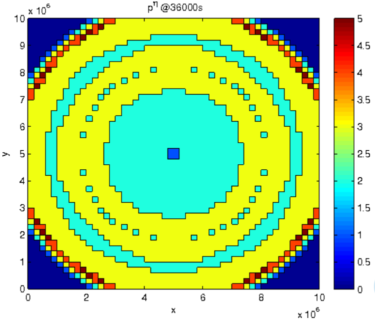

$f = 0$

Results at time 10 h; clockwise: η, η contours, local p^{eta}.

Maximum $C_{cel} = 2.23$.

Pure gravity wave (I): no rotation

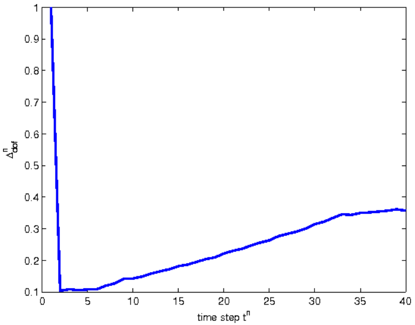

Fraction of degree of freedom *actually* used at *each* timestep:

$$\Delta^n_{dof} := \frac{\sum_{l=1}^{Nel}(p_l^\eta + 1)^2}{N_{el}(p_{max}^\eta + 1)^2}$$

Relative error on the celerity at different Courant numbers:

$\Delta t[s]$	C_{cel}	E_{cel}
150	2.2	2.34e-3
300	4.5	6.57e-2
600	9.0	1.80e-1

$$E_{cel} := \frac{\frac{(r^f_{peak} - r^i_{peak})}{(t^f - t^i)} - \sqrt{gH}}{\sqrt{gH}}$$

Geostrophic adjustment (I): f-plane

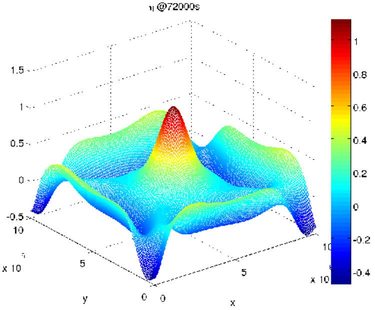

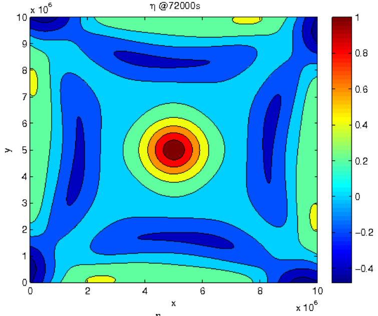

$f = f_0 = 10^{-4}$, (f-plane at midlatidudes)
Results at time 20 h; clockwise: η, η-contours, p^η.
Maximum $C_{cel} = 2.23$.

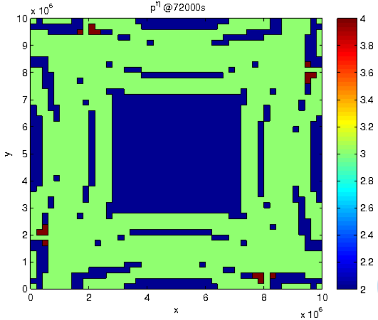

Geostrophic adjustment (I): f-plane

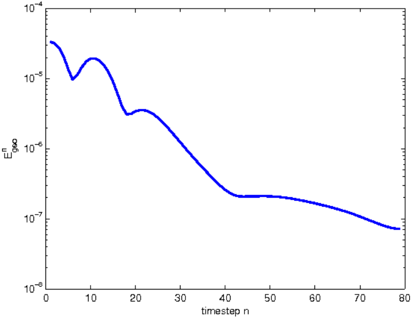

$\Delta t[s]$	C_{cel}	E^{geo}	E_{std}
225	0.55	3.03e-8	1.81e-7
450	1.1	2.99e-8	6.95e-7
900	2.2	2.98e-8	2.61e-6
1800	4.5	3.25e-8	8.98e-6

$$E_x^{geo} = \frac{1}{(\beta-\alpha)(\delta-\gamma)} \int_\alpha^\beta \int_\gamma^\delta \left| g\frac{\partial \eta}{\partial x} - fv \right| \; dxdy,$$

$$E_y^{geo} = \frac{1}{(\beta-\alpha)(\delta-\gamma)} \int_\alpha^\beta \int_\gamma^\delta \left| g\frac{\partial \eta}{\partial y} + fu \right| \; dxdy,$$

$$E^n_{geo} = MAX(E_x^{geo}, E_y^{geo})$$

Geostrophic adjustment (I): f-plane

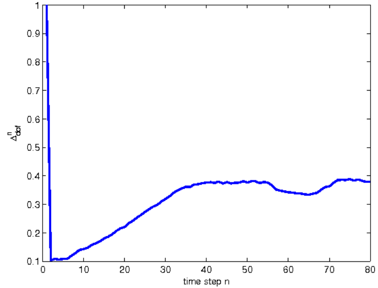

Fraction of degree of freedom *actually* used at *each* timestep:

$$\Delta^n_{dof} := \frac{\sum_{l=1}^{Nel}(p_l^\eta + 1)^2}{N_{el}(p_{max}^\eta + 1)^2}$$

Stommel gyre (I)

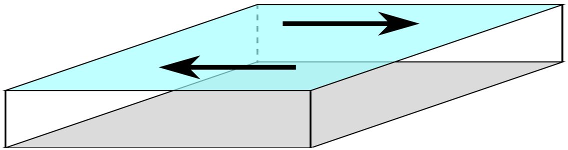

$$
\begin{aligned}
\partial_t \eta &= -\nabla \cdot (h\mathbf{u}) \\
\partial_t \mathbf{u} + \mathbf{u} \cdot \nabla \mathbf{u} &= -g\nabla\eta + f\mathbf{k} \times \mathbf{u} + \frac{\boldsymbol{\tau}^s}{\rho h} - \gamma \mathbf{u}.
\end{aligned} \tag{2}
$$

where

- $f = f_0 + \beta y, \quad f_0 = 10^{-4}, \quad \beta = 10^{-11}\mathrm{m}^{-1}$, (β-plane at midlatitudes)
- $\boldsymbol{\tau}^s = 0.1 \times sin(\pi y/L)\boldsymbol{e}_x$: wind stress.
- $\boldsymbol{\tau}^b = -\rho h \gamma \mathbf{u}$: linear dissipation term.

Simplest ocean basin model:

- no flux boundary conditions;
- not perturbed, zero velocity initial datum;
- square domain$(-L/2, L/2)^2, \quad L = 10^3 km$, covered with a regular mesh of 50×50 elements.

Stommel gyre (II): after two weeks

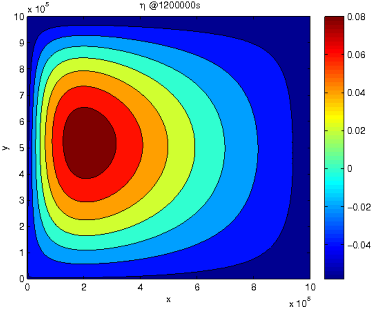

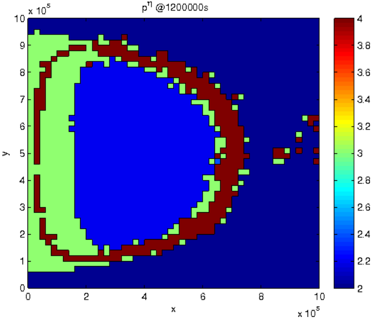

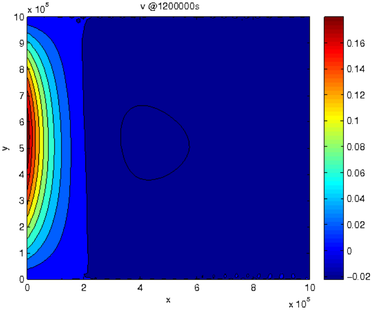

Results after two weeks, clockwise: η-contours, p^η and v.

Stommel gyre (III): after five weeks

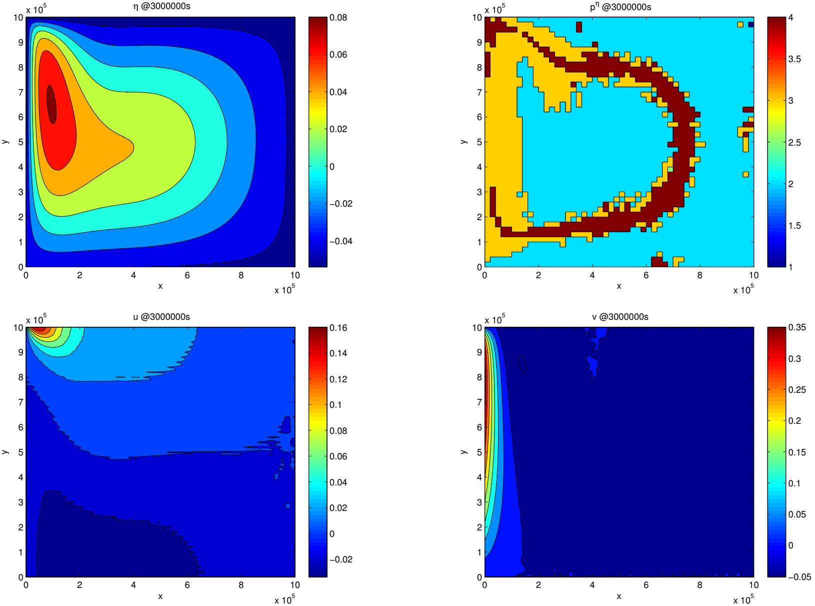

Conclusions and perspectives

- Summary:
  - A SISL DG discretization for rotating SWE has been presented, extending succesfully the SISL approach to DG framework.
  - Simple $p-$adaptivity approach allows to reduce the computational cost.
  - Numerical experiments in 1D and in 2D prove the effectiveness of the proposed approach.
  - Stability is studied considering the size of the maximum allowable Courant number.
- Open Issues:
  - Theoretical stability and dispersion analysis (on the way).
  - Coupling with conservative tracers advection (on the way).
  - Improvement of solver for SI step (preconditioning strategy).
  - Comparison with other stiff time integration techniques (e.g. Rosenbrock and exponential integrators).
- Future perspectives
  - Extension to the sphere (through introduction of suitable metric factors)
  - Use the presented SISLDG numerical technique to solve the Euler equations to develop a nonhydrostatic dynamical core for RegCM.

Thank you for your attention!